33rd Annual International Conference of the IEEE EMBS
Boston, Massachusetts USA, August 30 - September 3, 2011

Simulation and analysis of split gradient coil performance in MRI

Limei Liu, Hector Sanchez-Lopez, Michael Poole, Feng Liu, Stuart Crozier

Abstract —**Split magnet systems for hybrid imaging, such as positron emission tomography-magnetic resonance imaging (PET-MRI) and Radiotherapy-MRI, require gradient coils designed with similar shapes as their corresponding main magnet. This introduces challenges in the gradient coil design of good performance and manufacturing. In this paper the effect of the gap size in shielded transverse split gradient coils and split cryostat "warm" bore over the coil efficiency, shielding efficiency, wire spacing, cryostat ohmic power loss and mechanical vibration have been simulated and studied. A "free-surface" gradient coil design method was used to design the split, actively-shielded transverse gradient coils with an axial gap. A network method was used to calculate the eddy currents induced in the split cryostat "warm" bore. The shielding efficiency and the minimum wire spacing were found to decrease when the size of the central gap is increased. The ohmic power loss and the amplitude of the radial vibrations in the split cryostat "warm" bore increases when the gap size in the gradient coil and "warm" bore is increased. It is hoped that these investigations will be useful for the development of new hybrid imaging modalities involving MRI.**

I. Introduction

Recently, magnetic resonance imaging (MRI) has been combined with other imaging modalities. For example Positron Emission Tomography (PET)–MRI is designed to simultaneously produce complementary data aimed at early and accurate detection of tumours for cancer treatment [1], [2] and Radiotherapy-MRI is developed to accurately target therapy by using image guidance [3]. However, degradation of MRI system performance, particularly of the gradient coils, results from the combination of modalities that vie to occupy the same space [2], [3]. Splitting the MRI magnet and gradient coils assembly into two halves is one of the solutions to decrease the degradation [2], [3]. This split, hybrid configuration reduces the space available for the gradient coils [4] that, as a result, possess lower MRI performance. Conventional gradient coil design methods [5], restrict the current density to flow on a prescribed geometry such as cylinders and planes. Therefore as the gap increases the current-flowing surface is reduced. This results in regions of high current densities, undesirable hot spots and limited manufacturing reliability due to the minimal wire spacing between the coil conducting turns [6]. The state-of-the art in split gradient coils has a 3D structure which ameliorates some loss in gradient coil performance by connecting the primary and shield coil layers [7]. The coil performance is increased as a result of increased space provided for the gradient coils. Due to its proved geometric flexibility, an inverse boundary element method [8], [9] was used in the present work to design split gradient coils in order to study the gradient coil performance.

Another concern in MRI coil design is the eddy current induced in the surrounding conductive structures due to the switched gradient field. A network method proposed in [10] was used in this paper to simulate the eddy currents induced in the cryostat "warm" bore surface.

In the literature [4], [7], different central gap sizes have been used to insert PET sensors into the MRI scanner. In this paper the coil performance was studied by designing split coils with different gap sizes. The impact of the central gap size was studied and the competing requirements of maintaining a good gradient coil performance in a split MRI system were analysed and discussed. These data can be used to predict the coil performance for the development of new hybrid imaging modalities with MRI.

Gradient coil design is always a trade-off between different performance properties for any given geometry. As the size of the gap increases in the split system it is expected that; the coil efficiency will decrease, the accuracy of the magnetic field gradient will decrease, the inductance and resistance of the coil will increase and the amount of field reaching the cryostat of the magnet will increase due to the less effective active shielding. A derivative measure of coil performance, known as the figure-of-merit (FoM), which is the strength of the magnetic field produced by the gradient normalised by its inductance, is also expected to decrease with increasing gap size.

II. Methods

A. The design of actively shielded transverse gradient coils

An inverse boundary element method [8], [9] was used to design the 3D gradient coils. Fig. 1 (A) shows an example of the gradient coil surface incorporating a central gap. The radii of the primary and secondary surfaces were 34.4 cm and 43.5 cm, respectively and the total coil length was 135.6 cm. Primary and shield surfaces were connected at the ends furthest away from the region of interest (ROI). The axial length of the "warm bore" of the magnet cryostat was 170 cm, the inner radius was 50 cm and the thickness was 3.18 mm. In both sets of gradient coils studied in this paper, the gap size of the coil and "warm" bore was varied from 0 to 24 cm and the gradient field nonlinearity was constrained to 5% for all designs. For the vibration simulations, the mass density was 8000 kg/m^3, the Young's modulus was 193 GPa,

Manuscript received March 25, 2011

All the authors are with the School of Information Technology and Electrical Engineering, University of Queensland, Brisbane, QLD 4072, Australia

the effective frictional resistance K=100 Hz and the resistivity was 9.6×10^{-7} Ω·m.

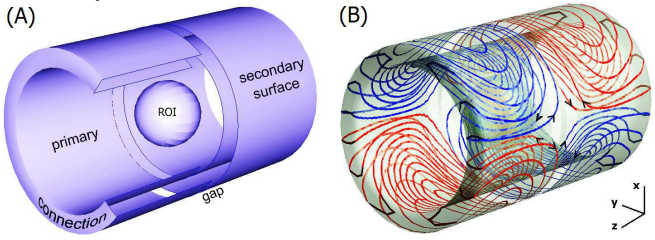

Fig. 1. (A) 3D representation of the gradient coil design surface. A section has been removed for better visualization of the coil surface and ROI. (B) One example of the transverse gradient coils. The arrows show the current directions.

To establish a fair comparison of performance as the gap size increases, two sets of coils were studied: a) coils that keep the same shielding efficiency when the gap is increased, termed "eddy coils"; b) coils that keep the same FoM when the gap is increased, termed "performance coils".

The shielding efficiency, γ, defined as

$$\gamma = 100\times\left(1-\frac{\max\left(\left|B_z^{eddy}\right|_{ROI}\right)/\max\left(\left|B_z^{coil}\right|_{ROI}\right)}{\left|B_z^{eddy\_ref}\right|_{ROI}/\left|B_z^{coil\_ref}\right|_{ROI}}\right) \quad (1)$$

where B_z^{eddy} and B_z^{coil} are the gradient fields at ROI produced by eddy current in the cryostat and the shielded gradient coils, respectively. $B_z^{eddy\_ref}$ and $B_z^{coil\_ref}$ are the gradient fields at ROI produced by the eddy current in the cryostat and the coil of the reference assembly, respectively. The shielding efficiency was fixed to γ=99% for all coils in the set a). With this simulated experiment it is intended to answer the following research question: **"what is the impact of the central gap size on the FoM for constant shielding efficiency?"**

The set b) was designed such that the FoM, η^2/L, was kept constant for all coils in the set. The inductance, L, dictates how fast the current in the coil can be switched on and off. The coil efficiency, η, is defined as the ratio between the magnetic field gradient strength and the operating current. The reference value of FoM was set to 9.5×10^{-6} $T^2\cdot m^{-2}\cdot A^{-2}\cdot H^{-1}$ produced by the coil without a gap. The question here was: **"how does the shielding efficiency reduce as the central gap increases if the FoM remains constant?"**

B. The network method for eddy current simulations

A network method was used to evaluate eddy currents induced in thick cylinders of finite length by coils of arbitrary geometry [10]. The method divides thick cylinders into layers thinner than the skin depth and expresses the surface current density as a weighted sum of normalized, truncated sinusoidal basis functions. The electromagnetic diffusion equation is solved by expressing the self inductance, mutual coupling and power dissipation using modified Bessel special functions and calculating the mutual coupling between the exciting source and the conducting cylinders in real space. The formulation presented in [10] can be extended to split cylinders if it is assumed that no current density is induced in the gap, which means the ρ component of the current density is zero.

In this study the annular conducting disks were not modelled which might connect the inner and outer cryostat cylinders and therefore it was assumed that the eddy currents are primarily induced in the axial cylinders. In order to support this assumption two models were built by FEMLAB (version 3.5, Comsol AB, Stockholm, Sweden) to simulate the current induced by 10 circular coils in a cylinder with and without disk connections. The network method was used to the case with no disk connections. The coils were driven by a harmonically varying current, $I(t)=I_0\cdot e^{i\omega t}$, with f = 1 kHz, I_0=2 A and $\omega=2\pi f$, and placed at z=±5 cm, z=±15 cm, z=±20 cm, z=±25 cm and z=±30 cm at the radius ρ=34.5 cm. In all the coils the current flew in the same direction. A cylinder of 3 mm thickness, 1 m axial length, 20 cm axial gap and 50 cm inner radius was used. The annual disks had a structure of 3 mm thickness, 50 cm inner radius, 90 cm outer radius, and were placed at z=±10 cm. The resistivity of the cylinder and disks was set to 3.1×10^{-8} Ω·m.

The FEMLAB model domain was discretized using 116355 triangular elements to obtain 5 layers in the radial direction of the cryostat. In the network method simulation the cylinder was also divided into 5 layers, hence the resulting layer thickness was 4.6 times smaller than the skin depth (δ=2.8mm at 1 kHz). The axial component of the magnetic field produced by the eddy currents was calculated along the radial axis at z=0 and ϕ=0 and the resulting values from FEMLAB and the network method were compared.

C. The string model for the cryostat vibration

Several parameters were simulated and analyses as a function of the central gap size. The string model, which was used to analyse the intensity and the tendency of the acoustic noise, has been successfully used to predict the mechanical vibration of x- and z-gradient coils [11] and has to be extended in the present study to evaluate the vibrations of the split cryostat "warm" bore. The ends of the strings were assumed to be fixed; hence no radial movement is induced in these points. These two parts of the split strings are symmetric with respect to z=0, they are not mechanically coupled and are considered as two independent oscillating systems. In this work the vibration of the "warm" bore was focused only. The gradient coil was driven by a sinusoidal current therefore the induced current oscillates with the same frequency [10]. The frequency, f, was varied from 0 to 25 kHz and the maximum value of the vibration amplitude was collected.

If the cylinder of axial length l is split into two symmetrical halves and the resulting gap is l_g then the amplitude of the radial vibrations (derived from Eq. (14) on page 35 of [11]) are expressed as

$$X_{Z\pm}(z,t)=\frac{16aB_0}{M}\sum_{n=1}^{\infty}\frac{F_{Z\pm}\sin\left(\frac{n\pi\left(z\mp l_g/2\right)}{l_g/2-l/2}\right)\exp(-i\omega t)}{(\omega+iK-\Omega_n)(\omega+iK+\Omega_n)} \quad (2)$$

where

$$F_{Z+} = \int_{l_g/2}^{l/2} J_\phi^+(z_0)\sin\left(\frac{n\pi(z_0 - l_g/2)}{l/2 - l_g/2}\right)dz_0 \quad (3)$$

and

$$F_{Z-} = \int_{-l/2}^{-l_g/2} J_\phi^-(z_0)\sin\left(\frac{n\pi(z_0 + l_g/2)}{l/2 - l_g/2}\right)dz_0 \quad (4)$$

where B_0 is the main magnetic field strength assumed here as 1.5 T, Ω_n is the frequency of the nth normal mode, M and a are the mass and radius of the split cylinder, respectively. $J_\phi^\pm(z)$ is the azimuthal component of the induced current density corresponding to the cylinder placed z>0 (+) and z<0 (-), respectively, which was calculated using the network method explained in section *B*.

The network method and (2) were implemented in Matlab (MathWorks, Natick, Massachusetts, U.S.A.). Coil design software coded in Matlab reports coil current pattern, FoM, wire space and gradient field linearity, while the network method reports the induced current density, axial magnetic field produced by the eddy currents at the ROI (B_z^{eddy}), power loss and mechanical vibration produced by induced currents.

III. Simulation Results and Discussions

A. Validation

Fig. 2 shows the model structures and the magnetic field simulated along the radial axis by FEMLAB and the network method, respectively. Fig. 2 (A) describes the model simulated using FEMLAB and the network method. Fig. 2 (B) shows the model with two radial disks simulated using FEMLAB. Fig. 2 (C) shows that the magnetic field values modeled with FEMLAB and network method are in good agreement for the points enclosed by the ROI (radius of the ROI was 20 cm).

A magnetic field deviation is more evident for the evaluation points close to the disks (40 cm up to 60 cm). This is due to the small portion of azimuthal current density that flows in the low corner of the disk close to the ROI. The good agreement of the network method with the values yielded by FEMLAB means that the network method can be used to predict the magnetic field produced by the eddy currents in the ROI and approximately evaluate the vibration induced in the split "warm" bore. The power loss calculated by FEMLAB (cylinder only) was 0.00262 watts and the power loss predicted by the network method was 0.00258 watts, which is in good agreement.

Fig. 1 (B) shows the wire pattern of one of the split transverse gradient coils. The wires are connected at the ends of the coil. The agreement between the simulations of cylinder only and cylinder with disks, shown in Fig. 2 (C), demonstrates that the ρ component of the current density induced in the radial disks (due to the connection of the coils end) and the ϕ component of the eddy current flowed from the cylinder to the disk are small and can be ignored.

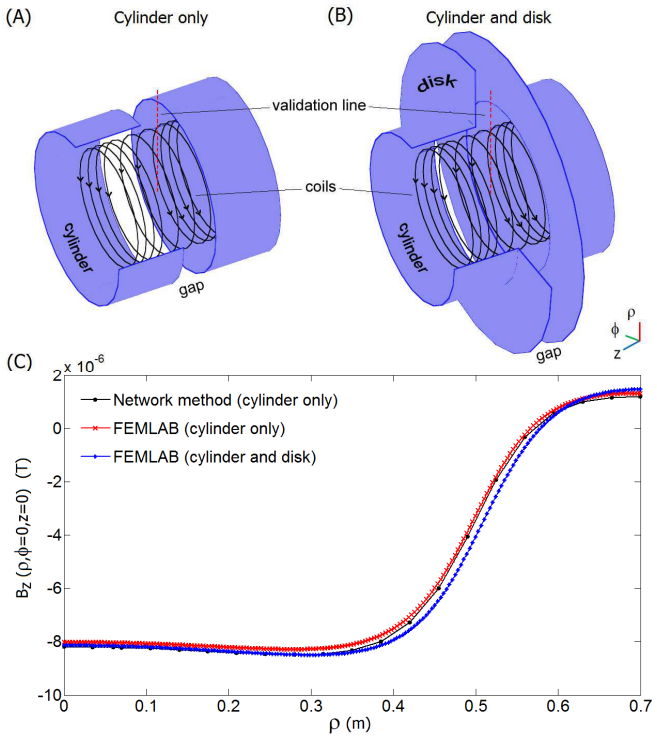

Fig. 2. (A) The "cylinder only" system modeled in FEMLAB. (B) The "cylinder and disk" system modeled in FEMLAB. A section has been removed for better visualization of the coils. The arrows show the current directions. (C) Axial component of the magnetic field produced by the eddy currents and evaluated along the radial axis ρ.

B. The coil performance analysis

Fig. 3 (A) depicts the behavior of the FoM for both experimental set a) and b) of coils as the gap size increases. When the gap size increased, the FoM tends to decrease for set a) designed to achieve 99% of shielding efficiency and 5% field linearity. This effect is due to limited surface area where the current density of the x-gradient coil is permitted to flow. As the gap increases, a current density with high frequency, oscillation appears in order to maintain 5% gradient field nonlinearity. Consequently the inductance tends to increase as the coil efficiency decreases (see Fig. 3 (B)). Another explanation for the FoM behaviour is that the coils were constrained to produce a target shielding efficiency when the gap size is increased. However, in Fig. 3 (B) the "performance coil" set b) shows an increase of the coil efficiency. This is a consequence of the reduction in shielding efficiency achieved by the coil design, when forced to maintain the FoM yielded by the shielded coil with no gap. (See Figs. 3 (A) and (C)). Essentially, with a gap size over 16cm with a FoM the same as no gap, the coils are completely unshielded.

Fig. 3 (C) shows that the shielding efficiency decreases, even for the coils designed to achieve 99% of shielding efficiency ("eddy coils" set a)). This is because the stream function represents the continuous current density with a limited number of wires, therefore the magnetic field produced by the primary coil leaks between the discrete wires of the shielding coil. If a more wires are used then this undesired effect would be reduced. The available space

where the current density flows is decreased when the gap size of the split coil support is increased. At the same time the distance between the ROI and the source current increases with the gap size, which implies that more current is required to produce the same target field strength and linearity.

Fig. 3 (D) depicts the gap size increasing as the minimum wire spacing decreases for both coil sets a) and b). The space limit is a big issue in coil performance. Coils with a high density of wires might induce temperature hot-spots and a special technique [12] may be used to spread the wires to avoid this issue. The temperature simulations [13] may help to see the change in peak temperature which needs to be modified to account for the central gap. .

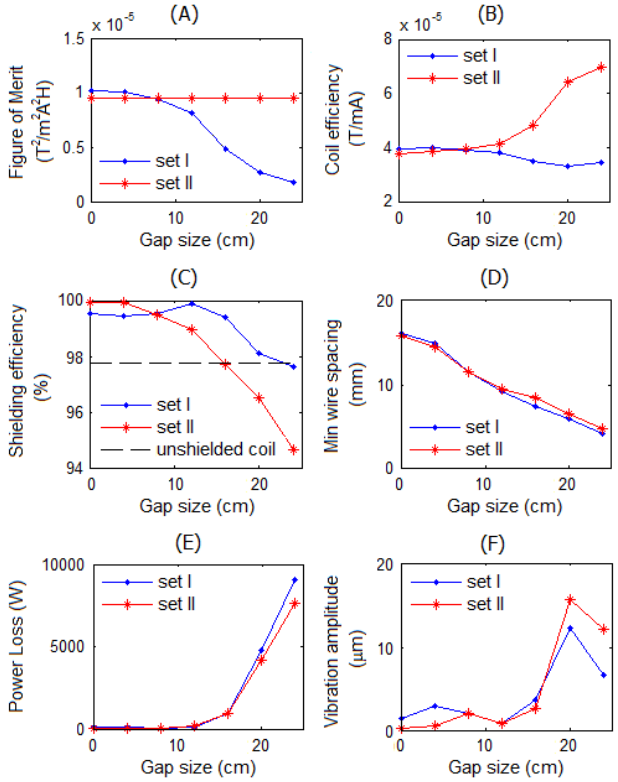

Fig. 3. Simulation results of the two coil sets. (A) FoM, (B) coil efficiency (η), (C) shielding efficiency, and the black dashed line is the reference shielding efficiency provided by an unshielded coil with no gap (D) minimum wire spacing, (E) cryostat ohmic power loss and (F) radial vibration amplitude in the split "warm" bore versus gap size.

Fig. 3 (E) shows that as the gap size increases, the ohmic losses in the split cryostat "warm" bore increases as a consequence of the reduction in the shielding efficiency. The power loss increases dramatically above 20 cm gap size; in these two last configurations the shielding is essentially non-existent as shown in Fig. 3 (C). It has been demonstrated that gradient coils designed with a constrained magnetic field generated by the eddy currents tend to have more power dissipation in the cryostat than coils designed with other shielding strategies [14].

Fig. 3 (F) shows that when the central gap increases, the amplitude of vibration tends to increase as a result of the reduction in shielding efficiency. However in the last case (gap 24 cm) the vibration tends to decrease due to the stiffness increment of the "warm" bore (short axial length).

IV. Conclusions

In this paper the effect on gradient coil performance as a function of the gap size in a split MRI system were simulated and studied. An inverse boundary element method was used to design the 3D transverse gradient coils. A network method was used to predict the eddy currents induced in the split cryostat without radial disk connections.

The gradient coil performance tends to decrease as the gap size of the split coil and "warm" bore increases, as expected. One important finding is that the FoM of set a) and the shielding efficiency of set b) decrease significantly for gap sizes more than approximately 16 cm. The cryostat power loss and vibration amplitude, used as the relative measure of acoustic noise, increases sharply over a 16 cm gap, indicate that the split system would be much louder than conventional systems. However, gap sizes below 16cm or the system studied here exhibit relatively acceptable levels of coil performance degradation.

In hybrid MRI systems, tradeoffs between the performance of MRI system and that of the other modality (PET or targeted radiotherapy, for example) have to be chosen carefully. In the present study it was found that when the gap is bigger than 16 cm the performance of the gradient coils reduced dramatically. However, the requirement for space for the other modality may outweigh this.

In the future work, a copper passive shield [15] may be attached to the split gradient assembly to improve the shielding efficiency in order to reduce the eddy current induced in the split "warm" bore cylinder.

References

[1] A.J. Lucas, *et al.*, *Technol Cancer Res Treat*, vol. 5, pp. 337–341, 2006.

[2] G. Delso and S. Ziegler, *European Journal of Nuclear Medicine and Molecular Imaging,* vol. 36, pp. 86-92, 2009.

[3] B. W. Raaymakers and et al., *Physics in Medicine and Biology*, vol. 54, p. N229, 2009.

[4] L.S. Petropoulos, M.A. Morich, *IEEE Trans. Magn.*, vol. 33, pp. 4107-4109, 1997

[5] R. Turner, Magnetic Resonance Imaging, vol. 11, pp. 903-920, 1993.

[6] S. Shvartsman, presented at the ISMRM 2010.

[7] M. Poole, et al., *Magnetic Resonance in Medicine*, vol. 62, pp. 1106-1111, 2009.

[8] S, Pissanetzky, *Measurement Science and Technology*, vol. 3, pp. 667-673, 1992

[9] M. Poole, R. Bowtell, *Concepts in Magnetic Resonance Part B: Magnetic Resonance Engineering*, vol. 31B, pp. 162-175, 2007.

[10] H. Sanchez Lopez, et al., *Journal of Magnetic Resonance*, vol. 207, pp. 251-261, 2010.

[11] D. Tomasi and T. Ernst, *Brazilian Journal of Physics*, vol. 36, pp. 34-39, 2006.

[12] M. Poole and et al., *Journal of Physics D: Applied Physics*, vol. 43, p. 095001, 2010.

[13] P. T. While, *et al.*, *Concepts in Magnetic Resonance Part B: Magnetic Resonance Engineering,* vol. 37B, pp. 146-159, 2010.

[14] M. Poole, *et al.*, *In press on IEEE transactions on applied superconductivity,* 2011.

[15] T. K. Kidane, et al., Magnetics, IEEE Transactions on, vol. 42, pp. 3854-3860, 2006.